Theoretical Study of Electronic Spectra of $[Pt_3(\mu\text{-}CO)_3(CO)_3]_n^{-2}$ (n = 3–5) Complexes

FERNANDO MENDIZABAL,[1] DARWIN BURGOS,[1] CLAUDIO OLEA-AZAR[2]

[1]*Departamento de Química, Facultad de Ciencias, Universidad de Chile, Casilla 653, Santiago, Chile*

[2]*Departamento de Química Inorgánica y Analítica, Facultad de Ciencias Químicas y Farmacéuticas, Universidad de Chile, Casilla 233, Santiago 1, Chile*

ABSTRACT: The platinum-platinum attraction and the spectroscopic properties of $[Pt_3(\mu\text{-}CO)_3(CO)_3]_n^{-2}$ (n = 3–5) were studied at the PBE level. Theoretical calculations are in agreement with experimental geometries. The absorption spectra of these platinum complexes were calculated by the single excitation time-dependent (TD) density functional method. All complexes showed MLCT transitions interrelated with the intertriangular complexes. The values obtained at the PBE level are in agreement with the experimental color range.

Key words: heavy atoms; electronic spectra; time-dependent

Introduction

Metal carbonyl clusters are of great interest as systems for catalytic reactions and they are potential contributors to some aspects of nanoscience and nanotechnologies such as molecular metal wires [1]. In particular, special attention has been devoted to the so-called "platinum carbonyl" of type Chini clusters [2–4]. They consist of triangular $[Pt_3(\mu\text{-}CO)_3(CO)_3]_n^{-2}$ complex fragments ($n \geq$ 1–10) stacked along the threefold axis of symmetry [2]. Since the mid-1970s, discrete oligomers with n = 1–5 have been characterized and studied theoretically [3, 4]. Recently, Longoni et al. have reported oligomers with n = 8 ($[Pt_3(CO)_3]_8^{-2}$) and $[Pt_{38}(CO)_{44}]^{-2}$ structures [5, 6]. Because of potential applications in molecular electronics and nanolithography, one has become to reinvestigation of the chemistry of Pt carbonyl clusters.

The minimum $[Pt_3(\mu\text{-}CO)_3(CO)_3]^{-2}$ dianion unit can be considered as a strong Lewis base, and there-

Correspondence to: F. Mendizabal; e-mail: hagua@uchile.cl
Contract grant sponsor: FONDECYT.
Contract grant number: 1060044 (Conicyt-Chile).

fore it can associate with neutral $[Pt_3(\mu\text{-}CO)_3(CO)_3]$ acting as a Lewis acid [4]. This mechanism allows to build that the 10 triangular clusters can be assembled through such interactions. The effect of growth is reflected in the different colors of the clusters in the solid state, e.g. $n = 3$, violet–green; $n = 4$, blue–green; $n = 5$, yellow–green [2, 3]. However, the UV-visible spectra have not been reported experimentally.

The study of bonding in the minimum triangular cluster unit has been enhanced by different theoretical methods at the Hückel Extended (EH), Hartree–Fock (HF) and density-functional levels [7, 8]. All the methods indicate that the orbital frontiers are formed from the *d* orbitals of platinum. It is clearly metal–metal bonding. At the HF level the optimization of the geometry of the $[Pt_3(\mu\text{-}CO)_3(CO)_3]_2^{-2}$ model has been reported. In this result the intermolecular Pt-Pt distance was 357 pm, longer than the experimental one of 304 pm [8]. This difference can be explained because the interaction between the triangular units is supported mainly by correlation effects via dispersion forces [9].

In general, when in the complexes studied there are two or more heavy atoms in a low oxidation state, they show evidence of metallophilic interactions. From the theoretical point of view, metallophilic attraction is considered as a correlation effect, strengthened by relativistic effects, and this phenomenon can be accounted [9, 10]. The mechanism underlying such attraction is the dispersion (van der Waals) interaction, with additional allowance for virtual charge-transfer terms [11]. The optical properties of molecules can be calculated from CIS and higher levels [12, 13]. In the last years the predicting power of density functional theory (DFT) with the time-dependent (TD) approach makes it the method of choice. There have been several reports of excellent agreement with experimental absorption and emission spectra in different platinum complexes [14, 15].

The aim of the present work is to study theoretically the triangular $[Pt_3(\mu\text{-}CO)_3(CO)_3]_n^{-2}$ ($n = 3$–5) complexes and relate the results to their excitation spectra. We propose to study the effect of several complexes and how their interactions can influence the spectroscopic absorption properties. To our knowledge, so far no systematic TD-DFT research has been done on these systems in order to explain their colors.

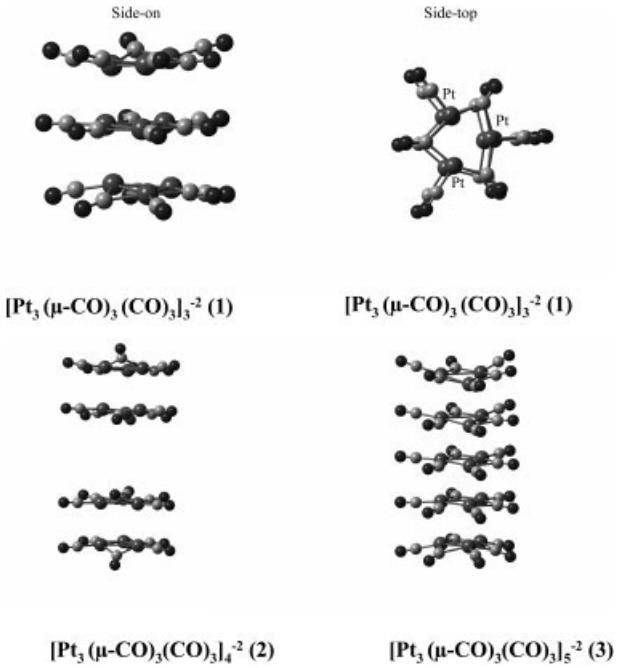

FIGURE 1. The $[Pt_3(\mu\text{-}CO)_3(CO)_3]_n^{-2}$ ($n = 3$–5) models (**1-3**).

Models and Methods

The $[Pt_3(\mu\text{-}CO)_3(CO)_3]_n^{-2}$ ($n = 3$–5) models used in our study are depicted in Figure 1. The geometries were fully optimized at the scalar relativistic PBE (Perdew–Burke–Ernzerhof)[16] levels in the gas phase. The optimization was performed within the C_{2v} point group in order to detect any tendency to intratriangular deviation from ideal D_{3h} symmetry. This effect was taken into account by Longoni in a model of $[Pt_3(\mu\text{-}CO)_3(CO)_3]_2^{-2}$ with good results [8].

We have used the PBE method because of reasonable previous results in the description of weak interactions and the electronic spectra. It is the best available functional for dispersion forces, without parameters fitted to experimental data. However, none of the existing functionals are optimal for evaluating the largely metallophilic dispersion contribution [17].

The excitation energies were obtained at the PBE level by using the time-dependent perturbation theory approach (TD-DFT) [18, 19], which is based on the random-phase approximation (RPA) method [20]. The TD-DFT calculations do not evaluate the spin-orbit splitting, and the values are averaged.

TABLE I

Main geometric parameters of the $[Pt_3(\mu\text{-}CO)_3(CO)_3]_n^{-2}$ (n = 3–5) systems (distances in pm and angles in degrees).

System	Method	Pt-Pt[a]	Pt-Pt[b]	PtC[c]	PtC[d]	CO[c]	CO[d]	PtPtPt[a]	PtPtPt[b]
$[Pt_3(\mu\text{-}CO)_3(CO)_3]_3^{-2}$ (**1**)	PBE	281	294	190	212	115	117	60.1°	168.5°
$[Pt_3(\mu\text{-}CO)_3(CO)_3]_4^{-2}$ (**2**)	PBE	283	306	189	210	115	118	60.2°	168.3°
$[Pt_3(\mu\text{-}CO)_3(CO)_3]_5^{-2}$ (**3**)	PBE	286	303	190	212	115	118	60.0°	177.6°
$[Pt_3(\mu\text{-}CO)_3(CO)_3]_n^{-2}$	Exp[e]	266–268	302–331	177–180	200–203	116	120		

[a] intratriangular Pt-Pt within each molecular unit.
[b] Intertriangular Pt-Pt between neighboring molecular units.
[c] CO terminal.
[d] CO bridging.
[e] Ref. [2].

The calculations were done using the Turbomole package (version 5.9) [21]. For Pt, the 18 valence-electron (VE) quasi-relativistic (QR) pseudo-potential (PP) of Andrae et al. [22] was employed. We used two *f*-type polarization functions on platinum (α_f = 0.70, 0.14) [14]. Also, the C and O atoms were treated through PPs, using double-zeta basis sets with the addition of one d-type polarization function [23]. The efficient resolution of the identity (RI) approximation was employed to obtain the final geometry and make the calculation feasible [24].

Results and Discussion

MOLECULAR GEOMETRY

We have fully optimized the geometries for the $[Pt_3(\mu\text{-}CO)_3(CO)_3]_n^{-2}$ (n = 3–5) models. Table I shows the main parameters, together with relevant experimental structural data. The theoretical results are in agreement with the experimental data when compared within each $[Pt_3(\mu\text{-}CO)_3(CO)_3]^{-2}$ unit. In all the models the platinum–platinum intratriangular distances are within the experimental range. The usual correlation-induced shortening is found for all systems, suggesting metallophilic attractions. This is clearly due to the effect of the ligands that remain joined to the platinum atoms in the basic units.

This situation changes when we compare the closest Pt-Pt intermolecular distances of the neighboring units. In all models there is an attraction. The Pt-Pt intertriangular distances obtained are 294, 306, and 303 pm in models **1–3**, respectively. It is worth noting that the PBE approximation overestimates the metallic interactions [10, 11]. This fact, may be due to the negative charge on each cluster. These results must be analyzed with caution, since DFT calculations do not describe properly the metallophilic attraction, although they can reproduce the metallophilic distance in some cases [9].

TIME-DEPENDENT (TD)-DFT CALCULATIONS

We calculated the allowed spin singlet transition for these systems, based on the ground state structures of models **1–3** at the PBE level. Only singlet–singlet transitions were considered in these quasirelativistic calculations. Here, we consider as permitted transitions those whose oscillator strength is different from zero. The allowed transitions obtained are shown in Figure 2 and Table II. The active molecular orbitals (MOs) in electronic transitions at the PBE level are shown in Figures 3–5.

Experimentally, there are no reported UV-visible spectra. However, the effect of growth is reflected in the different colors in the solid state that the clusters have, e.g. n = 3, violet–green; n = 4, blue–green; n = 5, yellow–green. This range of colors is in the wavelength between 650 and 490 nm.

The theoretical calculations are described in Table II. The calculated spectra of the three models (**1–3**) show principal transitions at 520, 557, and 660 nm, respectively, matching the experimental colors mentioned above (see Fig. 2). In the $[Pt_3(\mu\text{-}CO)_3(CO)_3]_n^{-2}$ (**1**) cluster the principal band at 520 nm is a mixture of excitations. The transition is composed mainly by $208a_1$ (dz^{2*}) $\rightarrow$ $219b_1$ (π^*), $206b_2$ (dz^{2*}) $\rightarrow$ $209a_2$ (π^*), and $207b_1$ (π) $\rightarrow$ $211a_1$ (π^*). This band corresponds to MLCT and LLCT. The active molecular orbitals in the electronic transition are shown in Figure 3. These results showed

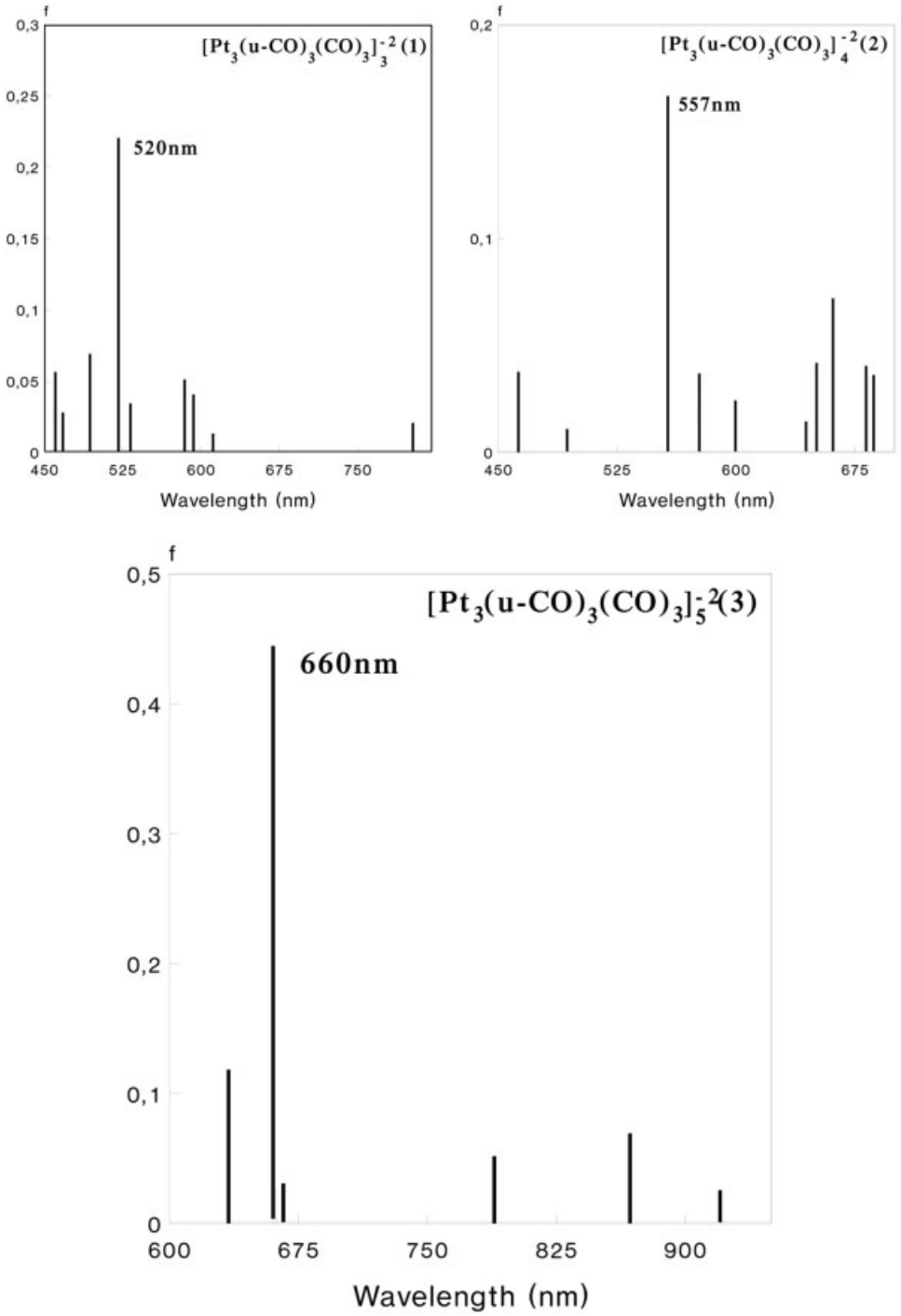

FIGURE 2. Calculated electronic PBE spectra of all the models.

that the charge transfers of the excitations take place mainly between the intertriangular platinum atoms.

When we used models **2** and **3**, a red shift of the excited bands and an increase in the transition intensity reflected in the magnitude of the oscillator strength were observed (see Table II). The bands are mainly a double MLCT of type $dz^{2*} \rightarrow \pi^*$, which can be understood from the MOs shown in Figures 4 and 5. A progressive shift in the wavelength of the

TABLE II

TD-DFT/PBE singlet-excitation calculations for $[Pt_3(\mu\text{-}CO)_3(CO)_3]_n^{-2}$ (n = 3–5).

System	Color	λ_{calc}/nm	f[a]	Contribution[b]	Transition type
$[Pt_3(\mu\text{-}CO)_3(CO)_3]_3^{-2}$	Violet–green	520	0.2206	$208a_1 \rightarrow 219b_1$ (21%)	MLCT ($dz^{2*} \rightarrow \pi^*$)
				$206b_2 \rightarrow 209a_2$ (20%)	MLCT ($dz^{2*} \rightarrow \pi^*$)
				$207b_1 \rightarrow 211a_1$ (18%)	LLCT ($\pi \rightarrow \pi^*$)
				$208a_1 \rightarrow 215b_1$ (13%)	MLCT ($dz^{2*} \rightarrow \pi^*$)
				$206b_2 \rightarrow 213a_2$ (7%)	MLCT ($dz^{2*} \rightarrow \pi^*$)
$[Pt_3(\mu\text{-}CO)_3(CO)_3]_4^{-2}$	Blue–green	557	0.1662	$265a_1 \rightarrow 278b_2$ (43%)	MLCT ($dz^{2*} \rightarrow \pi^*$)
				$271a_1 \rightarrow 278b_2$ (21%)	MLCT ($dz^{2*} \rightarrow \pi^*$)
				$267a_1 \rightarrow 278b_2$ (16%)	LLCT ($\pi \rightarrow \pi^*$)
				$277a_1 \rightarrow 284b_2$ (8%)	LLCT ($\pi \rightarrow \pi^*$)
				$277a_1 \rightarrow 287b_2$ (5%)	LLCT ($\pi \rightarrow \pi^*$)
$[Pt_3(\mu\text{-}CO)_3(CO)_3]_5^{-2}$	Yellow–green	660	0.4455	$284b_1 \rightarrow 290a_2$ (22%)	MLCT ($dz^{2*} \rightarrow \pi^*$)
				$286a_1 \rightarrow 298b_2$ (18%)	MLCT ($dz^{2*} \rightarrow \pi^*$)
				$284b_1 \rightarrow 289b_1$ (16%)	MLCT ($dz^{2*} \rightarrow \pi^*$)
				$286a_1 \rightarrow 293b_2$ (8%)	MLCT ($dz^{2*} \rightarrow \pi^*$)
				$285b_2 \rightarrow 287a_1$ (7%)	LLCT ($\pi \rightarrow \pi^*$)

[a] Oscillator strength.
[b] Values are $|coeff.|^2 \times 100$.

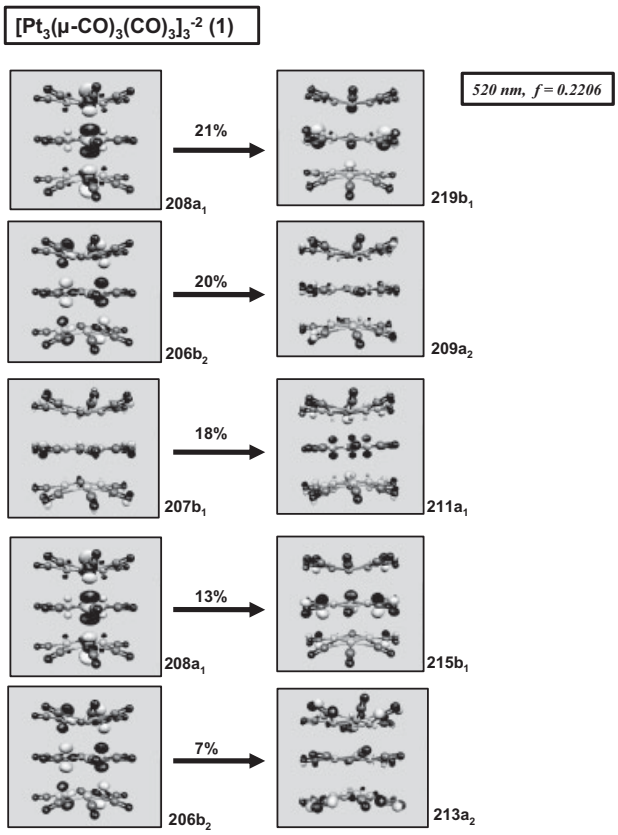

FIGURE 3. The active molecular orbitals in the $[Pt_3(\mu\text{-}CO)_3(CO)_3]_3^{-2}$ (**1**) electronic transitions at the PBE level.

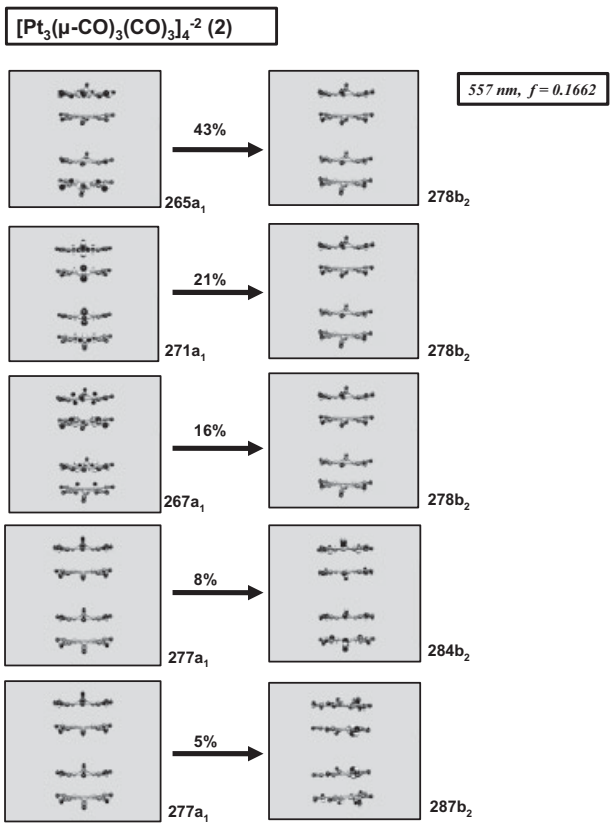

FIGURE 4. The active molecular orbitals in the $[Pt_3(\mu\text{-}CO)_3(CO)_3]_4^{-2}$ (**2**) electronic transitions at the PBE level.

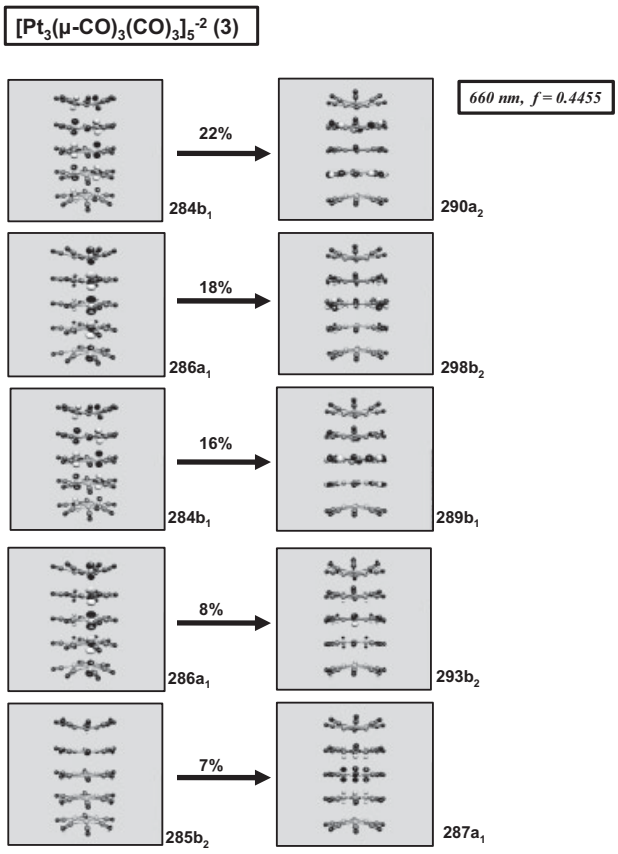

FIGURE 5. The active molecular orbitals in the $[Pt_3(\mu\text{-}CO)_3(CO)_3]_5^{-2}$ (**3**) electronic transitions at the PBE level.

excitation band from 557 nm (2) to 660 nm (3) took place by increasing the number of molecular units in the models. There is excellent agreement with the experimental color of the complexes. When the unoccupied orbitals were analyzed, we found a π bonding character between the neighboring molecular units.

Conclusion

This study provides further information on the nature of the platinum–platinum intra- and intermolecular interactions in the $[Pt_3(\mu\text{-}CO)_3(CO)_3]_n^{-2}$ (n = 3–5) complexes and on their spectroscopic properties. The idea was to show that it is possible to describe such properties through the clusters with several molecular units. The theoretical calculations are in agreement with experimental geometries. On the other hand, TD-DFT/PBE calculations clearly match the experimental color of the analyzed complexes. They show that intermetallic interactions are mainly responsible for the MLCT in models **1–3**, and they also present an LLCT component, which cannot be neglected. Also, there is a strong dependence between the intermolecular platinum–platinum contact in each system and the MLCT band, evidenced by a red shift effect at the experimental solid state level with the size of the cluster.

References

1. Femoni, C.; Iapalucci, M. C.; Kaswalder, F.; Longoni, G.; Zacchini, S. Coord Chem Rev 2006, 250, 1580.
2. Calabrese, J. C.; Dahl, L. F.; Chini, P.; Longoni, G.; Martinengo, S. J Am Chem Soc 1974, 96, 2614.
3. Longoni, G.; Chini, P. J Am Chem Soc 98, 1976, 7225.
4. Imhof, D.; Venanzi, L. M. Chem Soc Rev 1994, 23, 185.
5. Femoni, C.; Kaswalder, F.; Iapalucci, M. C.; Longoni, G.; Mehlstäubl, M.; Zacchini, S.; Ceriotti, A. Angew Chem Int Ed 2006, 45, 2060.
6. Femoni, C.; Kaswalder, F.; Iapalucci, M. C.; Longoni, G.; Mehlstäubl, M.; Zacchini, S. Chem Commun 2005, 5769.
7. Underwood, D. J.; Hoffmann, R.; Tatsumi, K.; Nakamura, A.; Yamamoto, Y. J Am Chem Soc 1985, 107, 5968.
8. Bengtsson-Kloo, L.; Iapalucci, C. M.; Longoni, G.; Ulvenlund, S. Inorg Chem 1998, 37, 4335.
9. Pyykkö, P. Chem Rev 1997, 97, 597.
10. Pyykkö, P.; Mendizabal, F. Inorg Chem 1998, 38, 3018.
11. Pyykkö, P. Angew Chem Int Ed Engl 2002, 41, 1001.
12. Zhang, H.-X.; Che, C.-M. Chem Eur J 2001, 7, 4887.
13. Pan, Q.-J.; Zhang, H.-X. Eur J Inorg Chem 2003, 4202.
14. Mendizabal, F. Int J Quantum Chem 2008, 108, 1164.
15. Pan, Q.-J.; Zhang, H.-X. Chem Phys Lett 2004, 394, 155.
16. Perdew, J. P.; Burke, K.; Ernzerhof, M. Phys Rev Lett 1996, 77, 3865.
17. Johansson, M. P.; Sundholm, D.; Vaara, J. Angew Chem Int Ed Engl 2004, 43, 2678.
18. Bauernschmitt, R.; Ahlrichs, R. Chem Phys Lett 1996, 256, 454.
19. Casida, M. E.; Jamorski, C.; Casida, K. C.; Salahub, D. R. J Chem Phys 1998, 108, 4439.
20. Olsen, L.; Jørgensen, P. In Modern Electronic Structure Theory; Yarkony, D. R., Ed.; World Scientific: River Edge, NJ, 1995; Vol. 2.
21. Ahlrichs, R.; Bär, M.; Häser, M.; Horn, H.; Kölmel, C. Chem Phys Lett 1989, 162, 165.
22. Andrae, D.; Häusserman, U.; Dolg, M.; Stoll, H.; Preuss, H. Theor Chim Acta 1990, 77, 123.
23. Bergner, A.; Dolg, M.; Küchle, W.; Stoll, H.; Preuss, H. Mol Phys 1993, 80, 1431.
24. Eichkorn, K.; Treutler, O.; Öhm, H.; Häser, M.; Ahlrichs, R. Chem Phys Lett 1995, 240, 283.